Impact of structural flexibility in the adsorption of wheat and sunflower proteins at an air/water interface

Alexandre Poirier, Amélie Banc, Romain Kapel, Martin In, Antonio Stocco, Laurence Ramos

Impact of structural flexibility in the adsorption of wheat and sunflower proteins at an air/water interface

Alexandre Poirier[1], Amélie Banc[1], Romain Kapel[2], Martin In[1], Antonio Stocco[1,3], Laurence Ramos[1]

[1] *Laboratoire Charles Coulomb (L2C), Univ. Montpellier, CNRS, Montpellier, France.*

[2] *Site Plateforme Sciences du Vivant et de la Santé, Laboratoire Réactions et Génie des Procédés (LRGP), 54500 Vandoeuvre-les-Nancy, France.*

[3] *Institut Charles Sadron, CNRS UPR22—University of Strasbourg, 23 rue du Loess, Strasbourg, 67034, France.*

Abstract

Food transition requires the replacement in human diet of animal-based proteins by alternative sources of proteins including plant-based proteins. This calls for a detailed knowledge of the functional properties of plant-based proteins, including their surface activity. In this framework, we provide here a comparative study of the interfacial properties of two plant proteins, extracted respectively from wheat and sunflower. We combine time- and concentration-dependent measurements of the surface tension and the surface rheology, as measured with a pendant-drop set-up, and of the surface excess concentration, as measured by ellipsometry, of plant protein interfacial films. We demonstrate a time-concentration superposition principle for the surface pressure and surface excess concentration, showing that the kinetics for the building of the interfacial films is essentially governed by the diffusion of the proteins from the bulk to the interface. We find that the rheological and structural properties of the interfacial protein films show markedly different behaviors for the two classes of protein, which is encoded in the structural features of the individual proteins: wheat proteins are more surface active than sunflower proteins, are keen to compress and re-arrange at an air-water interface, whereas sunflower proteins do not. This work provides qualitative and quantitative analysis of the comparative interfacial behavior of flexible and rigid plant proteins extracted respectively from wheat and sunflower, and demonstrates that a combination of several experimental techniques is necessary to obtain insightful information on the interfacial properties of any species.

Keywords: plant protein, surface tension, surface excess concentration, surface rheology, structure

1. Introduction

Adsorption of species on a solid or liquid interface is ubiquitous. Populating a liquid/liquid or a air/liquid interface with surface active species, as surfactants, colloidal particles, polymers and proteins [1, 2], impacts the surface tension of this interface. How the surface tension is reduced as a function of the amount of species adsorbed at the interface is not trivial, and depends on both thermodynamic and kinetic parameters. It is thus very useful to couple several techniques to measure concomitantly the amount of a surface active species at the interface and the properties of this interface, and derive quantitative equation of state, i.e. the link between the surface excess concentration and the surface pressure, in conjunction with the structural and mechanical properties of the interfacial film. Rich and complex behaviors are expected in the case for proteins that are prone to change conformations, gel or aggregate at a liquid/liquid interface. The structural rearrangements are multifactorial processes that are protein-specific and depend on intramolecular

interactions at the level of quaternary, tertiary and secondary structure [3]. In this context, proteins could be classified as rigid or flexible depending on their ability to undergo structural changes upon adsorption at an interface [4, 5]: a rigid protein would display a high internal stability which limits structural changes during adsorption contrary to a flexible protein that would show a low internal stability and could more easily undergo structural changes. However, this binary classification appears restrictive as for instance several globular rigid proteins can behave very differently at interfaces. Accordingly, some authors [6] have proposed to relate the behavior of proteins at interfaces to their thermodynamic stability using an instability index (*ii*); this index aims originally at predicting protein's metabolic stability in vivo in correlation with the amino-acid sequence [7]. In addition, recent experiments combining tensiometry with structural measurements of the interfacial films have demonstrated the coupling between the kinetics of the rearrangement processes of proteins at interfaces and the kinetics of adsorption of the proteins [8, 9]. The kinetics of adsorption depends on the diffusion of the proteins from the bulk to the interface, but can also be influenced by an adsorption barrier due to specific interactions between the species and the interface, as investigated for various proteins at air/water and oil/water interfaces [10]. To rationally account for the role of kinetics of diffusion from bulk to interfaces and check for accordance with a simple diffusive process, it is necessary to acquire data at different bulk concentration to assess the validity or the violation of a time-concentration superposition principle [5, 11, 12, 13, 14, 15].

On the other hand, current global challenges include feeding a growing population without damaging the planet, tackling the rise of diet-related diseases, and providing a diverse range of safe, tasty, and nutritious foods. These challenges call for a worldwide food transition towards more sustainable food products. It requires among other the replacement in human diet of animal-based proteins by alternative sources of proteins including plant-based proteins [16]. This calls for a deep understanding of the functional properties of plant-based proteins, in order to provide rational strategies for the replacement of animal proteins by plant proteins in conventional food. Functional properties include especially the ability to stabilize liquid interfaces, which is crucial for foams and emulsions (see for instance the recent review [17] and the references therein). Overall, plant proteins have been less investigated than their animal counterparts and the knowledge on the interfacial properties of plant proteins is considered rather scarce [18, 19].

In this work, we revisit some of our recently published results [20, 21] and add new experimental data and analysis for a comparative study of the interfacial properties of two food grade plant proteins, extracted respectively from wheat and sunflower, with contrasted behavior in bulk and at interfaces. The manuscript provides experimental data related to the bulk and interfacial structures. It is organized as follows. We first describe the materials and the techniques. We then present the experimental data focussing on the link between surface pressure, surface elasticity and surface excess concentrations, as gathered at different time and for different protein concentrations. We finally discuss the results that highlight similarities but also qualitative and quantitative contrasted features for the interfacial behavior of the two plant proteins, one from wheat being flexible with a high instability index and the other one from sunflower being more rigid with a lower instability index.

2. Materials and methods

2.1. Materials

Sunflower proteins are extracted from an industrial sunflower meal defatted by hexane, according to a protocol recently described by us [21]. In brief, we first use a solid-liquid extraction step mixing the sunflower meal with a 1 M NaCl aqueous solution and adjusting the pH at 7 by adding NaOH. The supernatant recovered after centrifugation is then purified by ultrafiltration and subsequently freeze dried. The protein extract comprises albumin and globulin with a globulin/albumin mass ratio of 4 as evaluated by chromatography. At pH 10 the net charge of globulins is 12 e^- and globulins are in their hexameric form with a molecular weight $M_w = 300$ kg/mol.

Wheat proteins are extracted from industrial gluten (courtesy of Tereos Syral, France) according to a protocol previously described by us [22, 23]. Briefly, gluten powder is mixed with 50% (v/v) ethanol/ water solvent and submitted to a continuous rotating agitation. After centrifugation, the supernatant is recovered

and placed at 4°C to induce a liquid-liquid phase separation. The light phase and the dense phase are separately recovered and freeze-dried. We use here the light phase, which is mainly composed of gliadins (78 % w/w gliadin, 15 % w/w large polymer-like glutenin and 7 % w/w small albumin and globulin [20]). The average molecular weight of gliadin is $M_w = 35$ kg/mol. Gliadins are monomeric proteins which are partially disordered; the unfolded domain comprises repetitive sequences rich in proline and glutamine residues and behaves like a flexible polymer chain [24].

To ensure a complete solubility of the proteins, sunflower proteins are dispersed in an aqueous solution containing 10^{-4} M NaOH (pH = 10), and wheat proteins are dispersed in a 50 mM acetic acid solution (pH = 3). Note that the two types of proteins are fully soluble in water only in a restricted range of pH. Quantitative reliable results can only be obtained for a pH in which the proteins are fully soluble. This prevents investigating wheat and sunflower proteins at a same pH and ionic strength. Samples are obtained by solubilizing the protein extract in the appropriate solvent. The suspensions are filtered with a 0.22 μm cellulose mixed ester membrane. The protein concentration C lies in the range $(0.05 - 10)$ g/L for sunflower proteins, and $(0.001 - 11)$ g/L for wheat proteins.

The diffusion coefficients of the individual proteins are measured by multi-angle dynamic light scattering for dilute suspensions ($C = 5$ g/L). We find $D = (35 \pm 5)$ μm^2/s for sunflower proteins, and $D = (45 \pm 10)$ μm^2/s for wheat proteins, yielding hydrodynamic radius $R_{\rm H} = \frac{k_{\rm B}T}{6\pi\eta D} = (6 \pm 1)$ nm for sunflower proteins and $R_{\rm H} = (5 \pm 1)$ nm for wheat proteins, assuming a spherical geometry for the proteins. Here $k_{\rm B}T$ is the thermal energy and $\eta = 1$ mPa.s is the solvent viscosity. Hence, the two proteins are characterized by markedly different density, evaluated as $\rho = \frac{M_w}{Nv}$, with M_w the average molecular weight of the proteins, N the Avogadro number, and v the volume of each protein which we take as $4/3\pi R_{\rm H}^3$. We find $\rho \simeq 110$ kg/m^3 for wheat proteins and $\rho \simeq 550$ kg/m^3 for sunflower proteins, considering the molecular weight of globulins. The different densities echoes the instability index (ii) of the two proteins, as computed using the ProtParam tool of Expasy using sequences P08079 for γ-gliadin and P19084 for sunflower globulin. The less dense wheat protein is also found as the less stable one: $ii = 109.79$ for proteins from wheat and $ii = 57.45$ for sunflower proteins.

We finally note that, for sunflower proteins, as shown later (Fig. 4), the time evolution of the surface excess concentration is quantitatively consistent with theoretical expectations when considering that the diffusion coefficient is the one of globulin, as measured experimentally by dynamic light scattering, hence showing that the main surface active components are globulins, which are also the major component in the extract.

2.2. Experimental techniques

2.2.1. Small and wide angle X-ray scattering

Small and wide angle X-ray scattering (SAXS and WAXS respectively) experiments are performed using an in-house setup of the Laboratoire Charles Coulomb, "Réseau X et gamma", Université Montpellier, France. The set-up comprises a high brightness low power X-ray tube, coupled with aspheric multilayer optic (GeniX 3D from Xenocs), which delivers an ultralow divergent beam (0.5 mrad, wavelength $\lambda = 0.15418$ nm). Scatterless slits are used to give a clean 0.6 mm diameter X-ray spot. The scattered intensity is collected on a two-dimensional Pilatus 300K pixel detector by Dectris (490×600 pixels) with pixel size 172×172 μm^2. The sample-detector distance is 1.9 m, respectively 0.2 m, for the SAXS, respectively WAXS, configuration. The scattered intensities are corrected for the sample transmission and the empty cell contribution. Samples, at protein concentration of 50 g/L are inserted in glass capillaries of diameter 1.5 mm.

2.2.2. Surface tension

We use a pendant drop tensiometer and a Wilhelmy plate set-up to measure the time evolution of the surface tension of an interface between air and an aqueous solution of protein. Experiments are performed at room temperature. The drop profile analysis tensiometer (PAT-1, SINTERFACE Technologies, Germany) is used in combination with surface rheology measurements. An aqueous drop is formed at the tip of a capillary (of diameter 2 mm). We use 15 mm^3 drops for experiments performed with wheat proteins,

and 30 mm^3 for experiments with sunflower proteins, in order to have the drop attached to the capillary independently of the protein type and concentration. Since the minimal surface tension for wheat proteins is lower, the drop volume is also lower. Generally, the size of the drop should be small enough, so that the drop is long-living, and large enough to have good rheological data and to maximize the accuracy of the drop contour fit. The chosen sizes meet these requirements. The images of the drop are recorded and the surface tension γ is computed from the shape of the drop [25]. We measure the surface tension over a period of one hour maximum after the formation of the drop. During this period, we have checked that the surface tension of the solvent is constant (γ_0=73 mN/m). A platinum Wilhelmy plate associated with a microbalance (KSV, Nima) is used in combination with ellipsometry measurements of the surface excess concentration (see below). The surface tension of a planar interface formed by an aqueous solution filling a glass Petri dish of 17 cm diameter is measured using standard methods [26]. In the presence of proteins, the surface tension γ is expected to vary with time and protein concentration, as the proteins adsorb at the air-water interface. Time 0 is the time of formation of the drop (when using a pendant drop tensiometer) or of the planar interface (when using a Wilhelmy plate).

2.2.3. Surface rheology

The pendant drop tensiometer (PAT-1M) is used to perform surface dilatational rheology measurements. The aqueous drop is subjected to small harmonic oscillations of its interfacial area A (of amplitude ΔA, such that $\frac{\Delta A}{A} = 5$ %), at a frequency of 0.1 Hz, leading to harmonic oscillations of the surface tension γ. The elastic and the viscous dilational modulus, E' and E'', are obtained by standard first harmonic analysis analysis [27].

2.2.4. Ellipsometry

To investigate the optical profile of the protein film at interfaces, an ellipsometer (Optrel, Germany) is used with a green laser (wavelength $\lambda = 533$ nm, Power 20 mW). The ellipsometric angles Δ and ψ, which are related to the ratio of reflection field coefficients are measured by nullying ellipsometry, at a unique incident angle $\varphi_{air} = 55$ deg. We have checked that, upon protein adsorption, the Brewster angle does not deviate from that of the bare interface, showing that measurements are performed in the limit of optically thin interfacial layers. In this regime, a perturbation theory can be used to extract from the measurements of the interfacial optical profile the surface excess concentration Γ (see [28, 29, 20, 21] for details). Measurements are performed in a Petri dish of diameter 17 cm. After gently pouring the protein solution in the dish, the interface is cleaned using a custom-made suction device. The completion of the cleaning step sets the time 0 of the measurements. The time evolution of the interfacial profile is measured for t in the range $(20 - 3600)$ s, respectively $(20 - 10000)$ s, for sunflower, respectively wheat, proteins. A food-grade transparent plastic wrap film with a small aperture is placed on the Petri dish to reduce evaporation, dusts and interface perturbation by draught.

3. Experimental results

3.1. Structure of the proteins in bulk

The markedly different density of the two proteins entails different structures in solution. The structure of individual proteins fully dispersed in solution is probed by X-ray scattering. We use rather dilute suspensions of the proteins ($C = 50$ mg/mL) to avoid interactions between proteins. We expect thus to probe the form factor of the proteins. The scattering profiles of the two types of proteins are different, reflecting differences in the structure of the proteins (Fig. 1). The wheat proteins display a scattering profile analogous to what is expected for random polymer coils: at large scattering vector q the scattered intensity I is measured to scale as q^{-2}, as expected for a polymer in a theta solvent [30]. The transition at low q toward a plateau is related to a characteristic size. A Guinier fit, $I \sim \exp(-\frac{R_G^2}{3}q^2)$ (black line in Fig. 1), gives a radius of gyration $R_G = 3.2$ nm, comparable to the size measured in dynamic light scattering. For the sunflower proteins, the scattering profile display more features. In particular the decrease at large q is modulated by several oscillations. Such oscillations associated with a lower level of scattering at high q point out

a denser structure of the sunflower proteins as compared to the wheat protein, at the corresponding $1/q$ scale. The positions of the successive extrema coincide with the ones of the form factor of a 5 nm radius sphere. However, the intensity scattered by a homogeneous sphere would be significantly lower than the one observed and this suggests a hollow structure as observed for other plant-based proteins such as globulin from rapeseed [31] and also soy glycinin [32]. Moreover the low q part of the scattering pattern of the sunflower protein clearly shows two characteristic lengths and suggests a bimodal population. To fit the scattering profile, we therefore consider a bimodal population of isotropic particles, with the large objects consisting of a Gaussian distribution of spheres with an average radius of 16 nm and a standard deviation of 4 nm, and the small objects consisting of hollow cylinders, with inner radius 1.3 nm, outer radius 4.7 nm and height 5 nm [33]. The resulting fit (thin black line in Figure 1) provides a reasonable good account of the experimental data. We find that the hollow cylinder population contributes to 20% of the scattered intensity at zero angle while the large spheres population contributes to 80%. Owing to the average volume of each population this corresponds to 8% in mass of large spheres, assuming a same density for the two types of objects. Hence, the largely dominant species are the small objects, whose size is comparable to that evaluated from the diffusion coefficient ((6 ± 1) nm), as measured by dynamic light scattering. On the other hand, we believe that the large objects, which are a minority species are small protein aggregates. The aggregates are not expected to contribute significantly to the surface tension properties because the aggregates are big, thus diffuse much more slowly to the interface. Furthermore, we expect the proportion of aggregates to decrease when the bulk concentration of protein decreases, hence to be even lower for the range of concentration investigated for the interfacial properties (C in the range $0.02 - 10$ g/L) than measured in the SAXS experiments ($C = 50$ g/L). Accordingly, the small proportion of protein aggregates will not be considered and discussed in the following.

Overall, X-ray scattering data are consistent with wheat proteins being very loose and akin to a polymer in theta-solvent, whereas the sunflower proteins are more compact globular proteins akin to dense colloidal particles.

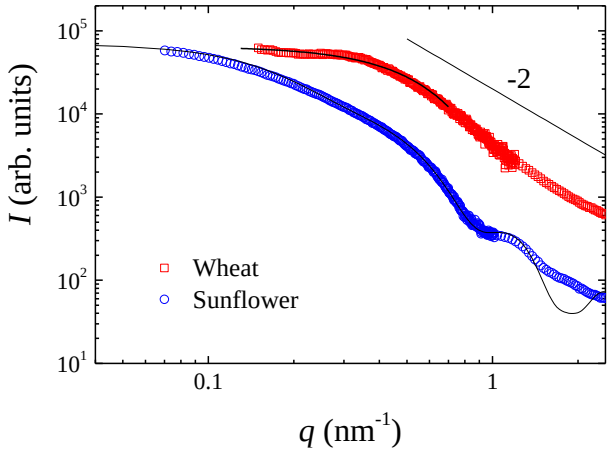

Figure 1. Scattered intensity profiles as measured by X-ray scattering for suspension of wheat proteins and sunflower proteins at concentration $C = 50$ mg/mL. Symbols are experimental data points. The thin black line is a fit of the data for sunflower proteins (see detail in the text), and the thick back line is a Guinier fit of the data for wheat proteins.

3.2. Link between surface pressure and surface viscoelasticity

We use a pendant drop set-up to measure the time evolution of the surface tension at the air/water interface, γ, for different protein concentrations, C, in the bulk. Data are plotted in terms of surface pressure Π defined as $\Pi = \gamma_0 - \gamma$, with γ_0 the surface pressure of the pure solvent ($\gamma_0 = 73$ mN/m). For both proteins, master curves of the surface pressure can be built when the time after the drop formation is

re-scaled by a concentration-dependent shift factor α. Master curves are obtained for concentration C in the range $(0.02 - 10)$ g/L for sunflower proteins and for C in the range $(0.1 - 11)$ g/L for wheat proteins. The two master curves (Fig. 2(a)) are qualitatively different, with more complex features for the one obtained for wheat proteins than for that obtained for sunflower proteins. For sunflower proteins, after a lag-time during which there is no measurable surface pressure, the surface pressure increases sharply before reaching a pseudo-plateau, at $\Pi_p \simeq (15 \pm 2)$ mN/m. At later times and/or higher concentrations, a second increase of the surface pressure is measured. As will be discussed below, surface elasticity (Figure 3) indicates that this second increase is linked to a time-dependent surface-induced aggregation of proteins. On the other hand, for wheat proteins, a multistep building of the interfacial film is evidenced. We find that the increase of the surface pressure after the lag-time is much smoother than for sunflower proteins. When Π reaches about 13 mN/m, a faster increase of Π is measured and followed first by a smooth increase of Π from 20 to 27 mN/m. Another sharp increase is measured at very long time and large concentrations, reaching surface pressures of the order of 40 mN/m. For the two types of proteins, the shift factor α is measured to vary as C^2 (Fig. 2(b)), demonstrating that the kinetics of building of the protein interfacial film are governed by the diffusion of the proteins from the bulk to the interface [11, 14, 20, 21]. The slight departure from the C^2 powerlaw observed at large concentration only for sunflower proteins reflects the aggregation of the proteins at the interface, which is linked the diffusion of the proteins from the bulk to the interface but is also kinetically driven. This process is more clearly evidenced when probing the surface elasticity and will be discussed below in association with the rheology data.

We measure that the onset of the surface pressure increase occurs more than one order of magnitude later for sunflower proteins than for wheat proteins. The lag-time before the surface pressure starts to increase is related to the diffusion of the protein from the bulk to the interface, but also to the surface activity of the proteins. Figure 2(b) demonstrates that the lag-time in both cases is related to diffusion-controlled adsorption. Nevertheless, despite similar bulk diffusion coefficients for the two proteins (we measure $D = 35 \pm 5$ μm^2/s for sunflower proteins and $D = 45 \pm 10$ μm^2/s for wheat proteins) drastically different lag-times are measured. This result indicates markedly different surface activities of the two proteins: wheat proteins are more surface active than sunflower proteins in the experimental conditions (in particular pH) investigated here.

Of note, a markedly different behavior is measured for wheat proteins at very small concentration: the lag time is followed by a very sharp increase of the surface pressure (Fig. 2), much sharper than for higher concentration (Fig. 2(a)). These data do not follow the master curve evidenced for higher concentration. Interestingly though, if we scale the data uniquely to get an overlap of the lag time, we find that the shift factor (empty dots in Fig. 2(b)) indeed follows the same scaling laws as the data gathered at higher concentration, showing that the onset of interfacial film is also governed by the diffusion of the proteins from the bulk to the interface. The markedly different behavior for low concentration wheat proteins is related to the combined effect of protein being depleted from the bulk and aging of the interfacial film. Given the finite size of the drop, we can evaluate the minimum bulk concentration $C_{\rm sat}$ to reach a full coverage (about $\Gamma_{\rm sat} = 3.1$ mg/mL, as shown below) of the drop interface (assuming that all proteins are located at the interface). From simple geometric arguments $C_{\rm sat} = \Gamma_{\rm sat} \frac{S}{V}$,with S and V respectively the surface and volume of the drop. For a drop of radius 1.5 mm, $C_{\rm sat} \approx 0.006$ g/L. This threshold concentration is comparable to the concentration below which departure from the master curve is measured. Hence for concentration below $C_{\rm sat}$, one would expect a plateau of the surface pressure. Instead we measure an increase of Π, which we believe is due to the aging of the film because of the rearrangement of the protein at the interface. The rearrangement processes are also a signature of the flexibility of the proteins. Note that reliable data at comparable small concentrations could not be obtained with sunflower proteins within the maximum duration time of the experiments, because of excessively long lag-times (about 2000 s for $C = 0.02$ g/L).

Surface rheology is also measured over time using the pendant drop set-up. We report in Figure 3 the evolution with the surface pressure of the elastic modulus E'. The loss modulus is always small as compared to the elastic modulus and will not be commented here. Over a certain range of surface pressure and protein concentration, data gathered at various protein concentrations are found to collapse on master curves. Overall we measure that the elasticity of sunflower proteins films is larger than the one of wheat

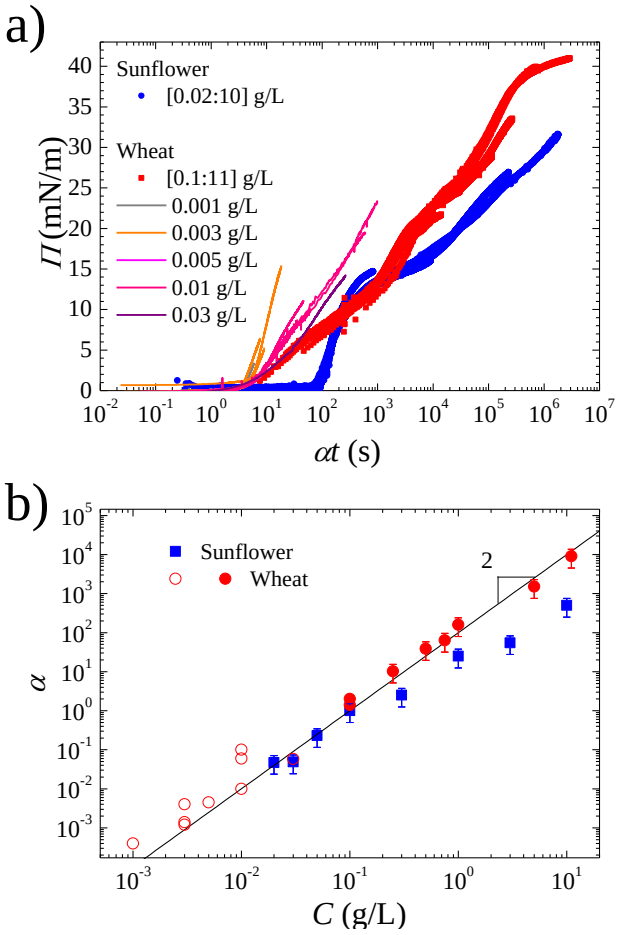

Figure 2. a) Masters curves obtained by plotting the surface pressure as a function of a normalized time, αt, using data with protein concentration $C = 0.1$ g/L as reference, for sunflower and wheat proteins. b) Scale factor α, as a function of C. The line is the theoretical expectation for a diffusive process. For wheat proteins the full symbols correspond to data obtained for C in the range $(0.1 - 11)$ g/L (red symbols in the master curves shown in (a)). Empty circles for wheat correspond to data obtained for lower concentrations that fail to collapse on the master curve (colored dashed lines in (a)).

protein films. Another marked difference is the fact that at high concentration and high surface pressure, the evolution E' for sunflower proteins does not follow a master curve but decreases as the bulk concentration C increases. This observation has been previously interpreted as the result of time-dependent interface-induced aggregation [21]. Note that the signature of this important effect on the elastic modulus is a weak departure from the C^2 scaling of the shift factor α for $C >\sim 1$ g/L (Fig. 2(b)).

A more quantitative analysis of the elastic modulus is provided below in the discussion section, where we focus our attention on the regime of relatively low surface pressures ($\Pi <\simeq 20$ mN/m).

3.3. Link between surface pressure and surface excess concentration

Additional and complementary information can be obtained by ellipsometry. Here, we concomitantly measure the variation of the surface excess concentration, Γ, and of the surface pressure, Π, of a flat air/water interface as proteins adsorb at the interface. The time evolution of the surface excess concentration is measured for different protein concentrations, for sunflower and wheat proteins. As for surface pressure measurements, data acquired at different concentrations collapse on a single curve once the time is re-scaled by the shift factor α. For sunflower proteins, data at low surface pressure and surface excess concen-

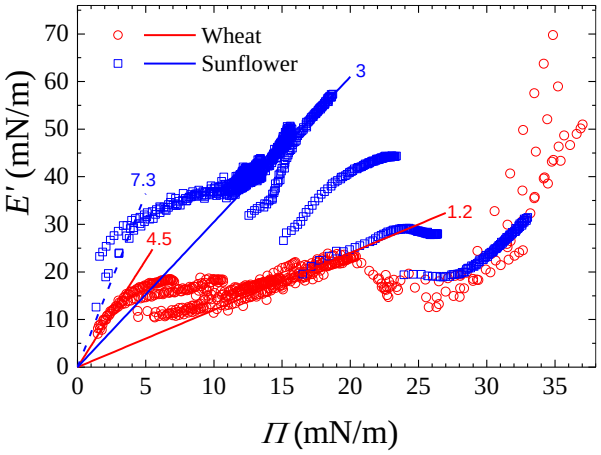

Figure 3. Dilatational elastic modulus E' as a function of the surface pressure for proteins from wheat and sunflower, as indicated in the caption. Symbols are data points. The continuous lines are affine fits of the data, at high surface pressure (for sunflower) and at low and high surface pressures (for wheat). The dashed line correspond to the expected behavior at low surface pressure for sunflower proteins based on the ellipsometry data (Fig. 5).

tration are considered, for which interface-induced aggregation is not relevant and the time-concentration superposition holds. The two sets of data gathered with wheat and sunflower proteins are qualitatively and quantitatively similar, showing an increase of the surface excess concentration that scales with the square root of time and is followed by a plateau regime. The data can be well fitted with the following functional form: $\Gamma = \Gamma_{\rm sat}\left[1-\exp\left(\frac{-2C}{\Gamma_{\rm sat}}\sqrt{\frac{Dt}{\pi}}\right)\right]$, which corresponds to an analytical modeling of a diffusion-controlled process with a saturation step [34, 35]. In rescaled units, the functional form reads: $\Gamma = \Gamma_{\rm sat}\left[1-\exp\left(\frac{-2}{\Gamma_{\rm sat}}\sqrt{\frac{DC_{\rm ref}X}{\pi}}\right)\right]$. Here, D is the bulk diffusion coefficient of the proteins, as measured by dynamic light scattering, and $X=\alpha t$, with $\alpha=(C/C_{\rm ref})^2$ and $C_{\rm ref}=0.1$ g/L. The best fits are shown in Figure 5, with $\Gamma_{\rm sat}$ the surface excess plateau as unique fitting parameter. The very good agreement between experimental data and theoretical prediction consistently demonstrates that the kinetics of protein adsorption is controlled by the diffusion of the proteins from the bulk to the air/water interface. Best fits yield $\Gamma_{\rm sat}=3.0$ mg/m^2 for sunflower proteins and $\Gamma_{\rm sat}=3.1$ mg/m^2 for wheat proteins.

From the surface excess concentration measured at saturation, one can evaluate the surface occupied by one protein at the interface as $S_{\rm sat}=\pi R_{\rm sat}^2=\frac{M_w}{\Gamma_{\rm sat}N}$ with M_w the average molecular weight of a protein, N the Avogadro number, and $R_{\rm sat}$ the average radius of the surface occupied by one protein at the interface. One finds $R_{\rm sat}=7$ nm for sunflower proteins, a value comparable to the hydrodynamic radius of the proteins as measured in the bulk ($R_{\rm H}=6\pm1$ nm). This suggests that the proteins are not deformed when saturating the air/water interface. By contrast, for wheat proteins, we find a significantly smaller value for $R_{\rm sat}=2.4$ nm, as compared to the hydrodynamic radius ($R_{\rm H}=5\pm1$ nm), suggesting that these proteins have the ability to deform and compress at the interface, yielding eventually to anisotropic organization of the gliadins (which display weakly elongated shape in bulk [20]).

By analogy with the master curves obtained by plotting the interfacial elastic modulus as a function of the surface pressure, Π (Fig. 3), we also find master curves when the surface excess concentrations is plotted as a function of Π. A plot of Γ vs Π provides useful information regarding the structure of the film. Such plots are displayed in Figure 5 for the two classes of proteins. Data at very low Π are very noisy but smoother and reliable measurements can be performed for Π larger than ~ 0.5 mN/m. Above this value, data collected at different protein concentrations collapse on a single curve. For sunflower proteins, a sharp increase of the surface pressure with Π is initially measured, which is followed by a plateau at $\Pi\simeq 9$ mN/m which starts for $\Gamma\simeq 3$ mg/m^2. For wheat proteins, the increase at small surface pressure is less sharp than for sunflower

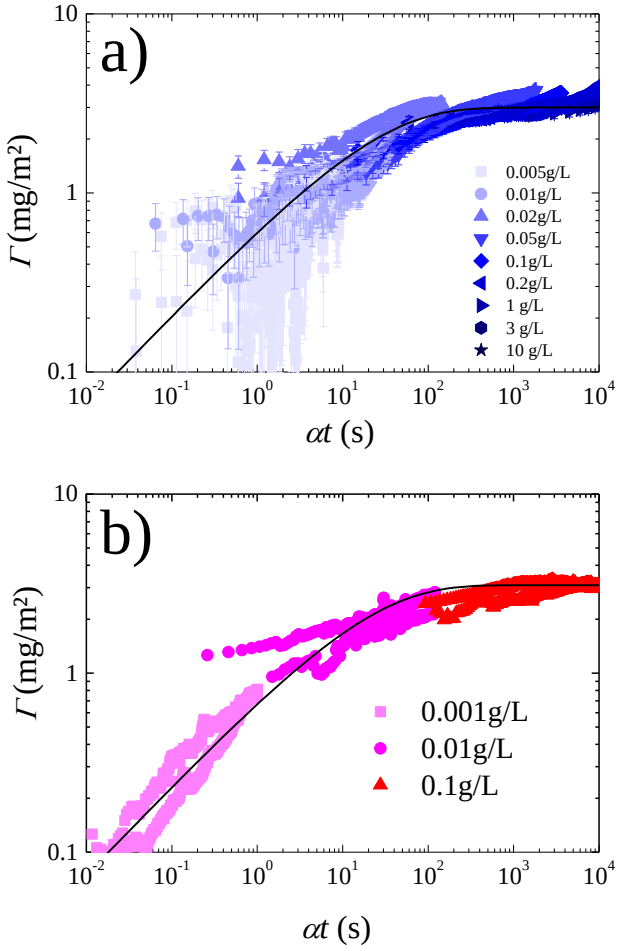

Figure 4. Surface excess concentration Γ as a function of the re-scaled time, αt, for proteins from sunflower (a) and wheat (b), at different bulk concentrations, as indicated in the caption. Symbols are data points and the lines are best fits. The reference concentration is $C = 0.1$ g/L.

proteins, and an even smoother increase of the surface pressure is measured for $\Pi > 5$ mN/m and $\Gamma > 1$ mg/m^2. Overall, data for wheat proteins appear shifted towards smaller surface excess pressure as compared to sunflower proteins, showing than less wheat proteins than sunflower proteins are required to reach a given surface pressure, hence confirming the higher surface activity of wheat proteins. This agrees with the data displayed in Figure 2 that show that wheat proteins induce an increase of the surface pressure at earlier times as compared to sunflower proteins, even if both proteins diffuse equally (since they have equivalent hydrodynamic radius). We believe that these observations are related to the fact that the wheat proteins spread more at the air/water interface, due to a higher flexibility. Consequently, the onset of the surface pressure at saturation occurs for a lower protein load at the interface for wheat proteins ($\Gamma_0 \approx 0.3 - 0.4$ mg/m^2) than for sunflower proteins ($\Gamma_0 \approx 1.5 - 2$ mg/m^2). An interesting parameter is to compare the value of the surface excess concentration at the onset of the surface pressure (Γ_0), with the excess surface concentration at saturation of the interface ($\Gamma_{\rm sat} \approx 3.1$ mg/m^2 for wheat proteins, and $\Gamma_{\rm sat} \approx 3$ mg/m^2 for sunflower proteins). This translates into a ratio between the surface occupied by each protein at the onset of surface pressure and at saturation, $A_{\rm max}/A_{\rm min} = \Gamma_{\rm sat}/\Gamma_0$, which quantifies the ability of wheat proteins to spread or compress at the interface, depending on the available surface. We find $A_{\rm max}/A_{\rm min} = 1.9 \pm 0.3$ for sunflower proteins. This value, closed to 1, is the signature of a rigid protein. By contrast, the significantly

larger values for wheat proteins, $A_{\max}/A_{\min} = 8.8 \pm 1.3$, is the signature of a flexible species that is able to largely deform and rearrange at the interface. Interestingly these numerical values are consistent with the ones found for well studied animal proteins: ($A_{\max}/A_{\min} \approx 2$) for a globular bovine serum albumin and ($A_{\max}/A_{\min} = 10$) for a more flexible β-casein [36, 37]. In these previous works, the evaluation was based on a complex modeling of the surface equation of state to account for surface elasticity vs Π, assuming that proteins adopt smaller molecular areas when increasing surface pressure.

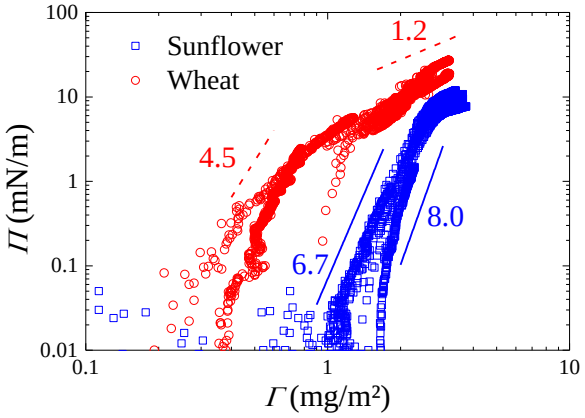

Figure 5. Surface pressure Π as a function of surface excess concentration Γ, as measured by ellipsometry, for proteins from wheat and sunflower, as indicated in the caption. Symbols are data points. The continuous line is a power law fit of the data at low surface pressure for sunflower proteins. The dashed line correspond to the expected behavior for wheat proteins, and for sunflower proteins at high surface pressure, based on the rheology data (Fig. 3).

4. Discussion and conclusion

We employ tensiometry, ellipsometry, and surface rheology to quantitatively study the adsorption of two plant proteins extracted from wheat and sunflower at a air/water interface. We use complimentary experimental data on the evolution of the surface elasticity and surface excess concentration with the surface pressure, and a Flory-like approach, as initially developed for polymers, to assess the conformation of the proteins at the interface [38, 39, 40]. In the semi-dilute regime at a liquid interface, we expect a scaling law for the surface pressure, Π, with the surface excess, Γ concentration $\Pi \sim \Gamma^p$. The exponent p is related to the solvent quality for the species at the interface and the 2 or 3-dimensional conformation of the proteins at the interface. In 2D (respectively 3D), $p = 8$ (resp. 3) for a theta-solvent, $p = 3$ (resp. 9/4) for a good solvent, and $p = 2$ (resp. 3/2) if the protein is fully extended. Operationally, the exponent p can be determined by ellipsometry, when the surface pressure and the surface excess concentration are concomitantly measured. It can also be obtained by surface rheology. Indeed, in the case of an essentially elastic interface, the elastic component $E' = \frac{\partial \Pi}{\partial \ln(\Gamma)} = p\Pi$. In this aspect, the combination of surface elasticity and surface excess concentration seems very useful to evaluate the structure of the proteins at the interface, because the two technics allow one to probe different regimes, at low surface pressure (Regime I) before reaching the interface saturation at $\Gamma_{\text{sat}} \approx 3$ mg/m^2, and beyond (Regime II). For sunflower the first regime at low Π is nicely measured by ellipsometry yielding an exponent $p = 7.3 \pm 0.7$. This value results from the independent fitting of two sets of data (see Fig. 5), and is fully compatible with the elastic measurement (see the two dashed lines in Fig. 3, which corresponds to slopes of 6.7 and 8). This indicates that in this regime the structure of the proteins is compatible with that of polymer species in a theta-solvent and the proteins form a two-dimensional layer. The second regime, which in fact is time-dependent and does not correspond to a thermodynamically stable state but instead results from protein aggregation, can only be measured by rheology. We evaluate p of the order of 3 for low protein concentration. This numerical value is in

agreement with proteins still in a theta-solvent but forming a 3-dimensional interfacial film. This finding is consistent to our expectation at the onset of protein aggregation, with protein aggregates nucleated at the interface and aggregates detaching from the interface and being released in the bulk aqueous phase. For wheat proteins, both regimes I and II by contrast obey time-concentration superposition and correspond to thermodynamic equilibrium state. In the first regime, we find $p \sim 4.5$ a significantly lower exponent than the one found for sunflower proteins, suggesting that wheat proteins form a two-dimensional film with species in good solvent condition. The exponent in regime II, $p = 1.2$ is very close to $p = 1.5$ that corresponds to a three-dimensional interfacial film for which the proteins can be considered as fully extended chains. The transition from regime I to regime II is therefore clearly associated to a structural rearrangement of the film. These results are in full agreement with the whole set of measurements.

Despite having comparable size in bulk the two proteins investigated are found to have different structures in solution, a sunflower protein being more compact than a wheat protein, and to behave markedly differently at an air/water interface. Our experimental results, which combine time- and concentration-dependent measurements of the surface pressure, surface elasticity and surface excess concentration, are consistent with the physical picture of wheat proteins being rather deformable entities, as opposed to more rigid and stable sunflower proteins. Comparative studies of the master curves for the time evolution of the surface pressure, Π, hint at a higher flexibility of wheat proteins. For wheat, the second increase of surface pressure is associated to a purely diffusive process, as opposed to the finding for sunflower proteins (see Fig. 2(b)). Moreover, the plateaus before and after the second increase of Π are poorly defined (as opposed to the case of sunflowers proteins). Finally, for surface pressures above the plateau, a unique master curve is obtained for the elastic modulus as a function of Π (for data acquired at different protein concentrations), suggesting that the surface pressure increase is a thermodynamic process whereas this is not the case for sunflower proteins. The many features of the time evolution of the surface pressure for wheat proteins is also the signature of the different rearrangement processes undergone by the wheat proteins at the air/water interface. Overall a larger elastic modulus is measured for sunflower proteins than for wheat proteins, for a given surface pressure, indicating also a more rigid species. Additionally, we find that the lag time for the onset of surface pressure up to a measurable level is much larger for the sunflower proteins than for the wheat proteins, although both proteins have equivalent bulk diffusion coefficient. This is due to a higher surface activity of wheat proteins, presumably due to their capability of spreading at the interface, in a regime of low coverage. In addition, we find that the wheat proteins are measured to be compressed when the interface is saturated by proteins, thanks to their flexibility.

Overall, our approach using master curves allows one to clearly highlight qualitative differences in the behavior of proteins, which are intrinsic to the structural features of the proteins, irrespective of their size hence of kinetics of adsorption.

Acknowledgements

This work was performed, in partnership with the SAS PIVERT, within the frame of the French Institute for the Energy Transition (ITE P.I.V.E.R.T., www.institut-pivert.com) selected as an Investment for the Future by the French Government under the reference ANR 10-IEED-0001. A.B. thanks the French National Agency for Research (ANR 18 CE06 001201) for teaching discharge. The authors thank Sara Albe Slabi and Odile Messieres for the extraction and the biochemical characterization of sunflower proteins, Marie-Hélène Morel for the development of the protocol for gliadin extraction, and Stéphane Pezennec for discussion.

References

[1] D. Möbius, R. Miller, Proteins at Liquid Interfaces, Elsevier, Amsterdam, 1998.
[2] E. Dickinson, Adsorbed protein layers at fluid interfaces: interactions, structure and surface rheology, Colloids and Surfaces B: Biointerfaces 15 (2) (1999) 161–176.
[3] L. Razumovsky, S. Damodaran, Surface activity-compressibility relationship of proteins at the air-water interface, Langmuir 15 (1999) 1392–1399.
[4] T. Arai, W. Norde, The behavior of some model proteins at solid-liquid interfaces 1. Adsorption from single protein solutions, Colloids and Surfaces 51 (1990) 1–15.

[5] B. C. Tripp, J. J. Magda, J. D. Andrade, Adsorption of globular proteins at the air/water interface as measired via dynamic surface tension: concentration dependence, mass-transfer considerations, and adsorption kinetics, Journal of Colloid and Interface Science 173 (1995) 16–27.

[6] V. Mitropoulos, A. Mütze, P. Fischer, Mechanical properties of protein adsorption layers at the air/water and oil/water interface: A comparison in light of the thermodynamical stability of proteins, Advances in Colloid and Interface Science 206 (2014) 195–206.

[7] K. Guruprasad, B. Reddy, M. W. Pandit, Correlation between stability of a protein and its dipeptide composition: a novel approach for predicting *in vivo* stability of a protein from its primary sequence, Protein Engineering, Design and Selection 4 (2) (1990) 155–161.

[8] P. A. Wierenga, M. R. Egmond, A. G. Voragen, H. H. de Jongh, The adsorption and unfolding kinetics determines the folding state of proteins at the air–water interface and thereby the equation of state, Journal of Colloid and Interface Science 299 (2) (2006) 850–857.

[9] Y. F. Yano, E. Arakawa, W. Voegeli, C. Kamezawa, T. Matsushita, Initial conformation of adsorbed proteins at an air–water interface, The Journal of Physical Chemistry B 122 (17) (2018) 4662–4666.

[10] T. Sengupta, L. Razumovsky, S. Damodaran, Energetics of protein-interface interactions and its effect on protein adsorption, Langmuir 15 (20) (1999) 6991–7001.

[11] F. MacRitchie, A. Alexander, Kinetics of adsorption of proteins at interfaces. Part I. The role of bulk diffusion in adsorption, Journal of Colloid Science 18 (5) (1963) 453–457.

[12] D. E. Graham, M. C. Phillips, Proteins at liquid interfaces, Journal of Colloid and Interface Science 70 (3) (1979) 12.

[13] M. Paulsson, P. Dejmek, Surface film pressure of β-lactoglobulin, α-lactalbumin and bovine serum albumin at the air/water interface studied by wilhelmy plate and drop volume, Journal of Colloid and Interface Science 150 (2) (1992) 394–403.

[14] C. Ybert, J.-M. Di Meglio, Study of protein adsorption by dynamic surface tension measurements: Diffusive regime, Langmuir 14 (2) (1998) 471–475.

[15] J. S. Erickson, S. Sundaram, K. J. Stebe, Evidence that the induction time in the surface pressure evolution of lysozyme solutions is caused by a surface phase transition, Langmuir 16 (11) (2000) 5072–5078.

[16] M. Springmann, M. Clark, D. Mason-D'Croz, K. Wiebe, B. L. Bodirsky, L. Lassaletta, W. de Vries, S. J. Vermeulen, M. Herrero, K. M. Carlson, M. Jonell, M. Troell, F. DeClerck, L. J. Gordon, R. Zurayk, P. Scarborough, M. Rayner, B. Loken, J. Fanzo, H. C. J. Godfray, D. Tilman, J. Rockström, W. Willett, Options for keeping the food system within environmental limits, Nature 562 (7728) (2018) 519–525.

[17] M. Nikbakht Nasrabadi, A. Sedaghat Doost, R. Mezzenga, Modification approaches of plant-based proteins to improve their techno-functionality and use in food products, Food Hydrocolloids 118 (2021) 106789.

[18] C. Berton-Carabin, K. Schroën, Towards new food emulsions: designing the interface and beyond, Current Opinion in Food Science 27 (2019) 74–81.

[19] S. Drusch, M. Klost, H. Kieserling, Current knowledge on the interfacial behaviour limits our understanding of plant protein functionality in emulsions, Current Opinion in Colloid & Interface Science 56 (2021) 101503.

[20] A. Poirier, A. Banc, A. Stocco, M. In, L. Ramos, Multistep building of a soft plant protein film at the air-water interface, Journal of Colloid and Interface Science 526 (2018) 337–346.

[21] A. Poirier, A. Stocco, R. Kapel, M. In, L. Ramos, A. Banc, Sunflower proteins at air–water and oil–water interfaces, Langmuir 37 (8) (2021) 2714–2727.

[22] M. Dahesh, A. Banc, A. Duri, M.-H. Morel, L. Ramos, Polymeric assembly of gluten proteins in an aqueous ethanol solvent, The Journal of Physical Chemistry B 118 (38) (2014) 11065–11076.

[23] M.-H. Morel, J. Pincemaille, L. Lecacheux, P. Menut, L. Ramos, A. Banc, Thermodynamic insights on the liquid-liquid fractionation of gluten proteins in aqueous ethanol, Food Hydrocolloids 123 (2022) 107142.

[24] L. Sahli, A. Boire, V. Solé-Jamault, H. Rogniaux, A. Giuliani, P. Roblin, D. Renard, New exploration of the γ-gliadin structure through its partial hydrolysis, International Journal of Biological Macromolecules 165 (2020) 654–664.

[25] J. D. Berry, M. J. Neeson, R. R. Dagastine, D. Y. Chan, R. F. Tabor, Measurement of surface and interfacial tension using pendant drop tensiometry, Journal of Colloid and Interface Science 454 (2015) 226–237.

[26] N. Wu, J. Dai, F. J. Micale, Dynamic Surface Tension Measurement with a Dynamic Wilhelmy Plate Technique, Journal of Colloid and Interface Science 215 (2) (1999) 258–269.

[27] F. Ravera, G. Loglio, V. I. Kovalchuk, Interfacial dilational rheology by oscillating bubble/drop methods, Current Opinion in Colloid & Interface Science 15 (4) (2010) 217–228.

[28] R. Toomey, J. Mays, M. Tirrell, In-situ thickness determination of adsorbed layers of poly(2-vinylpyridine)-polystyrene diblock copolymers by ellipsometry, Macromolecules 37 (2004) 905–911.

[29] A. Stocco, K. Tauer, S. Pispas, R. Sigel, Dynamics of amphiphilic diblock copolymers at the air–water interface, Journal of Colloid and Interface Science 355 (1) (2011) 172–178.

[30] R. H. Colby, M. Rubinstein, Polymer Physics, Oxford University Press, 2003.

[31] J. Pasquier, A. Brûlet, A. Boire, F. Jamme, J. Perez, T. Bizien, E. Lutton, F. Boué, Monitoring food structure during digestion using small-angle scattering and imaging techniques, Colloids and Surfaces A: Physicochemical and Engineering Aspects 570 (2019) 96–106.

[32] A. Sokolova, C. S. Kealley, T. Hanley, A. Rekas, E. P. Gilbert, Small-Angle X-ray Scattering Study of the Effect of pH and Salts on 11S Soy Glycinin in the Freeze-Dried Powder and Solution States, Journal of Agricultural and Food Chemistry 58 (2) (2010) 967–974.

[33] L. A. Feigin, D. I. Svergun, Structure Analysis by Small-Angle X-Ray and Neutron Scattering, Plenum Press, New York, 1987.

[34] A. F. H. Ward, L. Tordai, Time-dependence of boundary tensions of solutions I. The role of diffusion in time-effects, The

Journal of Chemical Physics 14 (7) (1946) 453–461.

[35] T. Miura, K. Seki, Diffusion influenced adsorption kinetics, The Journal of Physical Chemistry B 119 (34) (2015) 10954–10961.

[36] E. H. Lucassen-Reynders, V. B. Fainerman, R. Miller, Surface dilational modulus or Gibbs' elasticity of protein adsorption layers, The Journal of Physical Chemistry B 108 (26) (2004) 9173–9176.

[37] E. Lucassen-Reynders, J. Benjamins, V. Fainerman, Dilational rheology of protein films adsorbed at fluid interfaces, Current Opinion in Colloid & Interface Science 15 (4) (2010) 264–270.

[38] V. Aguié-Béghin, E. Leclerc, M. Daoud, R. Douillard, Asymmetric multiblock copolymers at the gas–liquid interface: phase diagram and surface pressure, Journal of Colloid and Interface Science 214 (2) (1999) 143–155.

[39] P. Cicuta, I. Hopkinson, Studies of a weak polyampholyte at the air–buffer interface: The effect of varying ph and ionic strength, The Journal of Chemical Physics 114 (19) (2001) 8659–8670.

[40] R. Douillard, M. Daoud, V. Aguié-Béghin, Polymer thermodynamics of adsorbed protein layers, Current Opinion in Colloid & Interface Science 8 (4) (2003) 380–386.